SCIENCE AND TECHNOLOGY ORGANIZATION
CENTRE FOR MARITIME RESEARCH AND EXPERIMENTATION

Reprint Series CMRE-PR-2019-132

Variable structure interacting multiple model algorithm for ship tracking using HF surface wave radar data

Gemine Vivone, Paolo Braca, Jochen Horstmann

June 2019

Originally published in:

OCEANS 2015, 18-21 May 2015, Genoa, Italy,
doi: 10.1109/OCEANS-Genova.2015.7271644

About CMRE

The Centre for Maritime Research and Experimentation (CMRE) is a world-class NATO scientific research and experimentation facility located in La Spezia, Italy.

The CMRE was established by the North Atlantic Council on 1 July 2012 as part of the NATO Science & Technology Organization. The CMRE and its predecessors have served NATO for over 50 years as the SACLANT Anti-Submarine Warfare Centre, SACLANT Undersea Research Centre, NATO Undersea Research Centre (NURC) and now as part of the Science & Technology Organization.

CMRE conducts state-of-the-art scientific research and experimentation ranging from concept development to prototype demonstration in an operational environment and has produced leaders in ocean science, modelling and simulation, acoustics and other disciplines, as well as producing critical results and understanding that have been built into the operational concepts of NATO and the nations.

CMRE conducts hands-on scientific and engineering research for the direct benefit of its NATO Customers. It operates two research vessels that enable science and technology solutions to be explored and exploited at sea. The largest of these vessels, the NRV Alliance, is a global class vessel that is acoustically extremely quiet.

CMRE is a leading example of enabling nations to work more effectively and efficiently together by prioritizing national needs, focusing on research and technology challenges, both in and out of the maritime environment, through the collective Power of its world-class scientists, engineers, and specialized laboratories in collaboration with the many partners in and out of the scientific domain.

Variable Structure Interacting Multiple Model Algorithm for Ship Tracking Using HF Surface Wave Radar Data

Gemine Vivone, Paolo Braca
NATO STO CMRE,
19126 La Spezia, Italy.
Emails: {gemine.vivone,paolo.braca}@cmre.nato.int

Jochen Horstmann
Helmholtz-Zentrum Geesthacht,
21502 Geesthacht, Germany.
Email: jochen.horstmann@hzg.de

***Abstract*—These last decades spawned a great interest towards low-power High-Frequency (HF) Surface-Wave (SW) radars for ocean remote sensing. By virtue of their over-the-horizon coverage capability and continuous-time mode of operation, these sensors are also effective long-range early-warning tools in maritime situational awareness applications. In this paper we show how it is possible to take advantage of *a priori* information on traffic by the means of a knowledge- based multi-target tracking algorithm, demonstrating that the tracking stage can be enhanced by combining on-line data from the HFSW radar with ship traffic information. A significant improvement of the proposed procedure, in terms of system performance, is demonstrated in comparison with the state-of-the-art approach recently presented in the literature. The main benefit of our approach is the ability to better follow targets without increasing the false alarm rate. The ability to follow targets can be over 30% better than existing methods. The proposed approach also exhibits a reduction of the track fragmentation. Average gains between the 13% and the 20% are observed.**

I. Introduction

Ship traffic monitoring represents one of the biggest challenges (*e.g.* in terms of law enforcement, search and rescue, environmental protection, and resource management) and, in the last years, it has led to intensive research activities in order to exploit existing sensor systems in support of maritime surveillance.

In this domain several monitoring assets can be exploited, from ground-based radar technologies to satellite sensors. However, it is important to take into consideration that many of these traditional solutions suffer from physical limitations, and only a smart integration of these different and often complementary systems can guarantee satisfactory performance. For instance, standard microwave radars operate only within line-of-sight propagation, with a maximum range of some dozens of kilometers, and satellite sensors (*e.g.* synthetic aperture radars) cannot grant a continuous temporal coverage of the region of interest.

High-Frequency (HF) Surface-Wave (SW) radar systems have been proposed as a cost-effective tool able to overcome many of these limitations. They can provide additional information on the vessel traffic, by virtue of their capability of detecting targets over-the-horizon, their continuous-time coverage, and their ability to estimate ship velocity through the Doppler data [1]. HFSW radars work in the 3-30 MHz band, with wavelengths between 100 m and 10 m, respectively. In this range, vertically polarized radio waves have the ability to propagate as surface waves. Low-power HFSW radar systems have been mainly developed for ocean remote sensing applications, *e.g.* surface currents and sea state mapping, wind extraction, wave spectra analysis and, recently, tsunami early-warning detection [2].

Few commercial systems based on the HFSW concept are available. They can be classified into two families [3]. The first one consists of high power systems of very large size and extension (usually exploited for military purposes). The second family is represented by systems that are typically used for environmental monitoring. The most common used systems are the Coastal Ocean Dynamics Applications Radar (CODAR), developed at National Oceanic and Atmospheric Administration (NOAA) [4], and the WEllen RAdar (WERA), developed at the University of Hamburg [5]. These systems are mostly operative on the coast. Compared to the systems in the first class, they transmit with significantly less power (< 50 W on average) and therefore, low electromagnetic pollution, but, unfortunately are less suited for ship detection and tracking [3].

Using HFSW radar system for target detection - a purpose for which there were not designed - poses additional challenges. Poor range and azimuth resolutions compared to microwave radars, high non-linearity in the state/measurement space, significant false alarm rate, due to both sea clutter and man-made/natural interference, and the crowding of the HF-spectrum [5] are all problems to cope with.

In previous works [6]–[8] some of the authors addressed these challenges with algorithmic approaches. A particularly promising approach [8] combines data from multiple radar stations. In that work, the signal processing chain consists of three stages: Detection, tracking, and fusion. The detection stage is performed using a 3D (range-azimuth-Doppler) Ordered Statistics (OS) Constant False Alarm Rate (CFAR) algorithm [9] developed at the University of Hamburg. The tracking part is based on the popular Joint Probabilistic Data Association (JPDA) rule [10], [11] in combination with the Unscented Kalman Filter (UKF) [12]. The data fusion strategy adopts the Track-to-Track Association and Fusion (T2T-A/F) paradigm [11].

Notwithstanding the good overall performance of these approaches, an analysis of the results reveals that track seg-

mentation (*i.e.* the generation of multiple tracker's tracks starting from an unique source target) remains a challenge. It is mainly due to the intermittent presence of the target contacts. Targets may be missing due to the radar synchronization being turned off, the target aspect angle or because of sailing into Bragg scattering regions [8], where ocean waves of half the radar wavelength travel toward and away from the radar site, causing intense scattering and, thereby decreasing the signal-to-clutter ratio and impeding target detections.

We note that the problem of track fragmentation in ship tracking is comparable to the problem of track obscuration in ground target tracking, where a moving target may become temporally obscured by tunnels or hills. In that case, the Variable Structure Interactive Multiple Model (VS-IMM) [13] has been proposed as a solution.

In this paper, we apply VS-IMM to the sea ship tracking problem borrowing it from the above-mentioned literature. We show that it yields improvements in three performances metrics: i) Time-on-Target (ToT); ii) False Alarm Rate (FAR); iii) Track fragmentation. Using both simulated and real data, we observed that the ToT improvements occur for any given value of the FAR, and can be in the 30% range; track fragmentation decreases by 13% - 20%.

The outline is as follows. The proposed target tracking methodology is presented in Sect. II. In Sect. III, the experimental results are reported. Finally, conclusions are drawn in Sect. IV.

II. Tracking Methodology

This section is devoted to the description of the tracking procedure applied to the HFSW radar for maritime traffic surveillance. This procedure is an enhanced version of the JPDA-UKF approach [8], which integrates the VS-IMM mechanism able to take advantage of the *a priori* information about historical ship traffic. The exploitation of this information in the tracking algorithm is a key input to this work, thus, a brief description of the ship traffic information is provided in the following section.

A. Ship Traffic Information

Ships and vessels exceeding a given gross tonnage are equipped with AIS transponders for position-reporting. Ships repeatedly broadcast their name, position and other details for automatic display on nearby ships. AIS reports contain both dynamic information (*e.g.* latitude, longitude, Course-Over-Ground (COG), Speed-Over-Ground (SOG)) and static information (*e.g.* vessel type, dimensions information).

Considering the historical AIS contacts of the area under study (see gray lines in Fig. 2), we note that there are some geographical regions where the traffic shows a certain regularity and where the maritime traffic is mostly concentrated. These are often called *sea lanes* or *routes*. The proposed tracking strategy is aimed at exploiting this kind of information to mitigate the problem of the target fragmentation (hence the name Knowledge-Based (KB) tracking). Similar conditions are present in the case of ground tracking, in which there are on-road targets following predetermined trajectories and off-road targets moving freely in the region. Analogously, a vessel can follow a route or can move more irregularly (for instance during fishing operations).

The KB tracking procedure, adopted here, integrates information about the ship traffic represented as a set of geographical sea lanes. We associate with each of them a specific dynamic model, as formalized in the following sections.

B. On/Off-sea lane Dynamic Models

The constant velocity model is adopted to describe the targets' dynamic [11]

$$\mathbf{x}_k = \mathbf{F}_k \mathbf{x}_{k-1} + \mathbf{\Gamma}_k \mathbf{v}_k, \tag{1}$$

where $\mathbf{x}_k = [x_k, v_{x_k}, y_k, v_{y_k}]^T$, x_k, y_k are the position components along X, Y directions, v_{x_k}, v_{y_k} are the corresponding velocity components, $[\cdot]^T$ is the transpose operator,

$$\mathbf{F}_k = \begin{bmatrix} 1 & T_k & 0 & 0 \\ 0 & 1 & 0 & 0 \\ 0 & 0 & 1 & T_k \\ 0 & 0 & 0 & 1 \end{bmatrix}, \mathbf{\Gamma}_k = \begin{bmatrix} T_k^2/2 & 0 \\ T_k & 0 \\ 0 & T_k^2/2 \\ 0 & T_k \end{bmatrix},$$

T_k is the current sampling time, $\mathbf{v}_k$ takes into account target acceleration and unmodeled dynamics, and is assumed to be Gaussian with zero-mean with covariance matrix $\mathbf{Q}_k$. We can define two different matrices $\mathbf{Q}_k$, depending on whether the motion is along sea lane or off a sea lane.

We handle the motion along a sea lane with the concept of "directional process noise" [13]. The standard motion models assume that the target can move in any direction and, therefore, use equal process noise variances in both the X and Y directions of the Cartesian system. This means that for off-sea lane targets the motion uncertainties in both directions are equal. For on-sea lane targets, the sea lane constraint means more uncertainty along the sea lane than orthogonal. Thus, the IMM module representing on-sea lane motion consists of process noise components along and orthogonal to the sea lane.

In the latter case, the motion model is matched with the direction of the sea lane ψ. From different sea lanes we have different values of ψ and therefore different models. In the off-sea lane target motion model, process noise components along X and Y directions are given by v_x and v_y, respectively. Variances of the noise components in the corresponding directions are given by σ_x^2 and σ_y^2, where σ indicates the standard deviation. Similarly, for the on-sea lane target motion model, the process noise component and its variance along the direction of the sea lane are given by v_a and σ_a^2, respectively. The corresponding values orthogonal to the sea lane are given by v_o and σ_o^2. Due to the higher motion uncertainty along the sea lane than orthogonal, we assume $\sigma_a >> \sigma_o$. This is a key element that is in contrast with the typical assumption $\sigma_x = \sigma_y$ used for the off-sea lane motion model, see, *e.g.* [8].

Starting from Eq. (1), we can have two categories of models by choosing different covariances of the Gaussian process noise at time k, *i.e.* $\mathbf{Q}_k$. The first one is:

$$\mathbf{Q}_k = \begin{bmatrix} \sigma_x^2 & 0 \\ 0 & \sigma_y^2 \end{bmatrix}, \tag{2}$$

with $\sigma_x^2 = \sigma_y^2$ used for the off-sea lane targets.

In the second case, since the state estimation is carried out in the X-Y coordinate system, the variances of the process noise components along and orthogonal to the sea lane need to be converted into the covariance matrix. Thus, we have [13]

$$\mathbf{Q}_k = \begin{bmatrix} -\cos\psi & \sin\psi \\ \sin\psi & \cos\psi \end{bmatrix} \begin{bmatrix} \sigma_o^2 & 0 \\ 0 & \sigma_a^2 \end{bmatrix} \begin{bmatrix} -\cos\psi & \sin\psi \\ \sin\psi & \cos\psi \end{bmatrix}. \tag{3}$$

Sect. II-D establishes the method selecting the proper motion dynamic based on the on-line data gathered from the radar.

C. Observation Model

Assuming a radar located at the origin in spherical co-ordinates, the target-originated measurement equation can be expressed as

$$\mathbf{z}_k = \mathbf{h}\left(\mathbf{x}_k\right) + \mathbf{n}_k, \tag{4}$$

the radar measures the target range, bearing (azimuth), and range rate, then Eq. (4) can be recast as follows

$$\begin{aligned} \mathbf{z}_k &= \left[z_k^r, z_k^b, z_k^{\dot{r}}\right]^T, \\ \mathbf{n}_k &= \left[n_k^r, n_k^b, n_k^{\dot{r}}\right]^T, \\ \mathbf{h}\left(\mathbf{x}_k\right) &= \left[h_r(\mathbf{x}_k), h_b(\mathbf{x}_k), h_{\dot{r}}(\mathbf{x}_k)\right], \\ h_r(\mathbf{x}_k) &= \sqrt{x_k^2 + y_k^2}, \\ h_b(\mathbf{x}_k) &= \arctan\left(\frac{y_k}{x_k}\right), \\ h_{\dot{r}}(\mathbf{x}_k) &= \frac{x_k v_{x_k} + y_k v_{y_k}}{\sqrt{x_k^2 + y_k^2}}, \end{aligned} \tag{5}$$

where $z_k^r, z_k^b, z_k^{\dot{r}}$ are radar measurements of the target range, bearing, and range rate. The measurement noise vector $\mathbf{n}_k$ is assumed to be Gaussian with zero-mean and covariance matrix $\mathbf{R}_k$ given by

$$\mathbf{R}_k = \begin{bmatrix} \sigma_r^2 & 0 & \rho\sigma_r\sigma_{\dot{r}} \\ 0 & \sigma_b^2 & 0 \\ \rho\sigma_r\sigma_{\dot{r}} & 0 & \sigma_{\dot{r}}^2 \end{bmatrix}. \tag{6}$$

Note that in literature [11], [14], n_k^r,n_k^b,$n_k^{\dot{r}}$ are all assumed to be statistically independent, except for n_k^r and $n_k^{\dot{r}}$, which are correlated with a correlation coefficient ρ defined as in [15].

D. VS-IMM Estimator

We exploit the VS-IMM estimator in the case of a generic r^{th} target. The possible modes are given by all the on/off-sea lane dynamics described in Sect. II-B. Clearly, we have as on-sea lane modes all the identified maritime routes.

It is assumed that the generic target r evolves according to one of the modes at time k. The mode-conditioned state estimate and the associated covariance of the filter module j_r are denoted by $\hat{\mathbf{x}}_k^{j_r}$ and $\mathbf{P}_k^{j_r}$, respectively. The steps of the VS-IMM estimator are detailed in [13], [16].

E. Adaptive Filter Module Selection

1) Entry/Exit Conditions: When an off-sea lane target enters the vicinity of a sea lane, it could become an on-sea lane target. Similarly, a target on a sea lane may leave it. Unlike an off-sea lane target, which is free to move in any direction, the motion of an on-sea lane target is highly directional along the sea lane. In view of the highly directional motion of on-sea lane targets, when it is determined that an off-sea lane target is in the vicinity of a sea lane, a new mode, representing motion along that sea lane, is added to the mode set. Similarly, a decision is made as to whether the considered target leaves the vicinity of a sea lane, in the case the related mode is removed.

One of the major issue in adding or deleting modes to handle on-sea lane/off-sea lane motion is deciding when to add or delete, *i.e.* how to determine that a target enters or leaves a sea lane. Thus, at time k, for each established track r, a decision is made about which sea lanes the target can follow. This is carried out by testing whether the predicted location lies within a certain neighborhood ellipsoid of any sea lane (for instance, neighborhood ellipsoids for the real cases can be seen in Fig. 2). A problem of the above decision process is that the target has several modes at time $k-1$ with their own predicted states and covariances and consequently there is not a unique state/covariance prediction. A possible solution is that if at least one of these predicted states lies inside the ellipsoid then we add the related sea lane mode. At each time interval a sea lane neighborhood test is carried out for each track against all the sea lanes defined. Modes corresponding to sea lanes not validated are removed from the mode set. Using the above validation strategy, entry into or exit from sea lanes is handled by the estimator.

2) Obscuration Conditions: Assume that a target follows a given sea lane and, for some reason (such as, the first order Bragg scattering or radar synchronization), it is not visible (no detections are associated). Then, some *a priori* information needs to be exploited in order to obtain the target state estimate, its covariance, and the filter likelihood. The UKF state estimate and the VS-IMM equations do not take into account the target visibility, *i.e.*, they assume that the target is always visible. When a track follows the sea lane mode and there are no associated observations then the estimator is defined as follows.

The filter module corresponding to that sea lane is replaced with a "hidden target" model that modifies the filter estimates and likelihoods using the information that the target detection probability P_D is zero. The hidden-target model is similar to the "dead-target" model [11] that is commonly used for track termination. The hidden target model accounts for the event that the target has become not visible. For this model, the state estimate of the target r under the mode of the j^{th} sea lane at time k, *i.e.*, $\hat{\mathbf{x}}_k^{j_r}$ and the associated covariance $\mathbf{P}_k^{j_r}$, are given by:

$$\hat{\mathbf{x}}_k^{j_r} = \hat{\mathbf{x}}_{k|k-1}^{j_r}, \tag{7}$$

$$\mathbf{P}_k^{j_r} = \mathbf{P}_{k|k-1}^{j_r}, \tag{8}$$

where $\hat{\mathbf{x}}_{k|k-1}^{j_r}$ and $\mathbf{P}_{k|k-1}^{j_r}$ are the predicted estimate and its covariance under the mode j of the target r at time k as classically defined in the UKF prediction equations, see [12], [17].

Since no detection is used in the state estimate, a similar modification is required in evaluating the filter likelihood, which quantifies, in the VS-IMM estimator, the filters confidence in the measurement. The following expression is used for the likelihood of the hidden target r under the mode of the j^{th} sea lane at time k:

$$\Lambda_k^{j_r} \stackrel{def}{=} \frac{1}{V}, \tag{9}$$

where V is the filter gate volume given by

$$V = \gamma^{n_z/2} V_{n_z} |\mathbf{S}_k^{j_r}|^{1/2}, \tag{10}$$

and V_{n_z} is the volume of the unit hypersphere of dimension n_z, n_z is the cardinality of the measurement $\mathbf{z}$ (*i.e.* 3 in this case), γ is the gate size used for the measurement validation (equal to 5) and $\mathbf{S}_k^{j_r}$ is the innovation covariance of the target r under the mode j_r at time k. For radar measurements with range, azimuth and range rate, $V_{n_z} = \frac{4\pi}{3}$ [11]. For the "hidden target" model, which treats the measurement as a spurious one, V^{-1} is the filter clutter density λ in its validation gate.

The "hidden target" model is removed from the mode set if one of the following conditions become true: i) the target becomes visible again; ii) the corresponding sea lane segment is no longer validated.

F. Data Association: The Multiple Model JPDA

The VS-IMM approach makes the assumption that for each target in each frame a measurement is present. In that case, the measurement is used to update the target track. However, in multi-target tracking scenarios in presence of target missed detections and false alarms, it is necessary to decide which one of the received measurements should be used to update a particular track. Hence, a data association mechanism (measurement-to-track association) is required. In this paper the multiple model JPDA algorithm is exploited to cope with this issue, for details see [16], [18].

G. Track Management

The adopted track management strategy is briefly resumed below:

- The M-of-N rule is used for the track initiation [11], [16]. If the M-of-N rule's requirements are satisfied, the track becomes a *confirmed track*. Otherwise, it is dropped;
- A confirmed track is said *on-sea lane confirmed track* if the target that is generating the track follows the same on-sea lane mode for a period time (*i.e.* it has as main mode an on-sea lane one, at least, for a certain number of scans W) otherwise it is defined *off-sea lane confirmed track*;
- An on-sea lane confirmed track is terminated if one of the following event occurs:
  - The likelihood in Eq. (9) goes down a given threshold τ;
  - The counter that takes into account the number of consecutive scans in which the target is not visible exceeds a given value NNT_{max};
  - The target's track uncertainty (state covariance matrix) has grown beyond a certain threshold;
  - The target has reached an unrealistic maximum velocity v_{max}.
- An off-sea lane confirmed track is terminated if one of the following event occurs:
  - No detection has been validated for the past M^* out of N^* most recent sampling times;
  - The target's track uncertainty (state covariance matrix) has grown beyond a certain threshold;
  - The target has reached an unrealistic maximum velocity v_{max}.

III. Experimental Results

In this section a comparison between the proposed VS-IMM JPDA and the standard JPDA is provided by using both simulated and real data of HFSW radar systems. As already proposed in [8], we use as ground truth for tracking assessment the AIS static/kinematic reports. AIS ship reports are checked in order to remove possible outliers, missing position reports, and unreliable data.

The association procedure between radar and AIS contacts considers that the time intervals between the AIS reports and the radar timestamps are not aligned. Thus, we have to interpolate the kinematic AIS reports in the HFSW radar timestamps. Then, the association is carried out by searching for the nearest among all the radar tracks which fall in the performance validation region centered on the AIS contact.

Some performance metrics, already introduced in [8], are here described and used. The normalized Time-on-Target (ToT) is defined as the ratio between the length of an active track (correctly associated to the AIS) and the AIS track length. The ideal value is equal to 1. The False Alarm Rate (FAR) is determined as the number of false track contacts, normalized with the recording interval and the area of the surveyed region. A false alarm is defined as a contact that does not belong to any AIS report. The ideal value is 0 (no false alarm). Finally, the number of radar tracks N^{TF} associated with a single target is an index that measures the Track Fragmentation (TF). An ideal system would have $N^{TF} = 1$, *i.e.* the radar system is able to follow the whole track without loosing it.

The main parameters of the proposed VS-IMM JPDA tracking algorithm can be divided in the following groups:

- *IMM* - The probability to switch from the off-sea lane to an on-sea lane mode and vice versa is 0.05;
- *Model* - For the dynamic models, the sampling period T_k is 16.64/33.28 s. The standard deviation process noise parameters for the off-sea lane mode are $\sigma_x = \sigma_y = 0.01$ m/s^2 while for an on-sea lane mode are $\sigma_o = 0.001$ m/s^2 for the component in the sea lane orthogonal direction and $\sigma_a = 0.01$ m/s^2 for the component in the along sea lane direction. The process noises related to the observation model are the same for all the modes. The standard deviation in range (σ_r) is 150 m, in azimuth (σ_b) is 1.5°, and in range rate ($\sigma_{\dot{r}}$) is 0.1 m/s;
- *Hidden* - The likelihood threshold τ is set to 0.001, the maximum number of scans for which the target

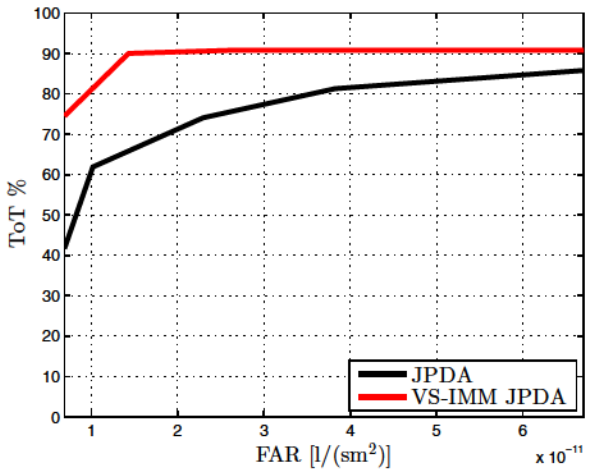

Fig. 1. ToT Vs. FAR varying N^* using a number of MC runs 10^3.

can be unobservable NNT_{max} is set to 25. In order to add the "hidden target" model, the number of scans W in which an on-sea lane mode has to be the most likely is set to 5;

- *Logic* - The maximum target velocity v_{max} is set to 20 m/s. Furthermore, M is chosen to be equal to 5 while N is 6. Furthermore, we choose $M^* = N^*$ in the off-sea lane track termination logic. N^* will be specified for each test case;
- *Detection* - The detection probability P_D is set to 0.35 and the clutter density λ is 10^{-9} m^{-2}.

In the following, the outcomes on both simulated data and real data will be shown.

A. Simulation Results

The analysis is related to the behavior of the VS-IMM JPDA and the standard JPDA varying the parameter N^*. The results are obtained by averaging 10^3 Monte Carlo (MC) trials. Half of the simulated target trajectories follows the sea lane and are generated accordingly to the directional noise dynamic model described in Sect. II-B. The others do not follow the sea lane and are generated accordingly to the off-sea lane dynamic model, see again Sect. II-B. Then, the radar plot is generated in a uniform cluttered environment with a detection probability $P_D = 0.6$. We report the relationship between the ToT and FAR in Fig. 1 for the VS-IMM JPDA and the standard JPDA. It is worth noting that when the parameter N^* grows, the FAR and the ToT increase. We have that the VS-IMM outperforms the standard JPDA in terms of ToT/FAR. In other words, for each value of the FAR, we obtain that the ToT of the VS-IMM is higher than the one of the standard JPDA. Furthermore, we point out that in the region where the FAR is small, that represents the most important region form an operative point of view, the performance gap between the two approaches is larger.

B. Real Data Performance Assessment

The proposed KB-tracking has been tested on whole dataset provided by the NURC BP09 experiment starting from May 7, 2009 to June 4, 2009. Data from the Palmaria and S. Rossore WERA radar systems (named *Palmaria* and *S. Rossore* datasets) have been separately processed using the CFAR algorithm developed at the University of Hamburg. The detections are then provided to the KB-tracking and to the standard JPDA [8] for comparison purposes. Fig. 2 depicts the selected areas to test the two approaches.

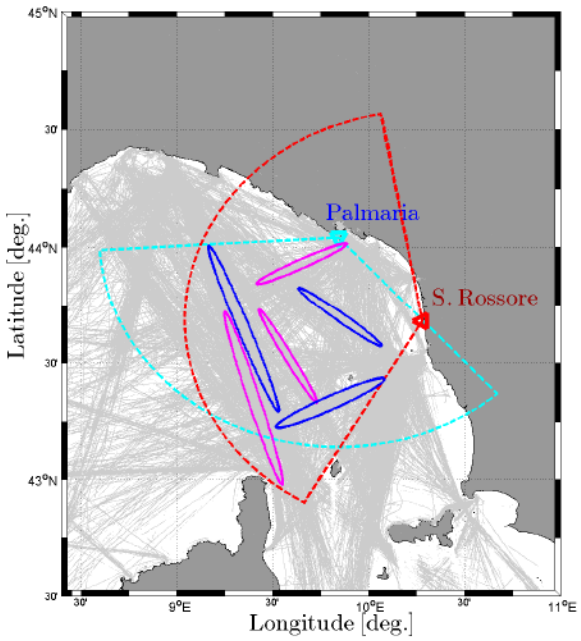

Fig. 2. Real case scenario: In red and cyan the S. Rossore and Palmaria radar fields of view. Magenta ellipsoids indicate the selected areas for the S. Rossore dataset, while, in blue the ones for the Palmaria dataset. Gray lines represent the historical AIS trajectories.

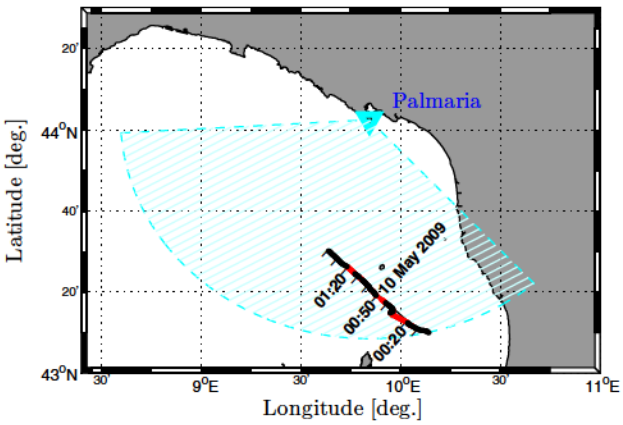

Fig. 3. Graphical representation of the VS-IMM JPDA fragmentation reduction with respect to JPDA using the same track management parameters. Tracks generated from both the JPDA and VS-IMM JPDA are depicted in black, while the tracks generated only by the VS-IMM JPDA are depicted in red.

In Fig. 3 an example of the two approaches under test is

TABLE I. MEANS ON BOTH THE DATASETS FOR TOT AND FAR INDEXES.

(a) Palmaria

N^*	JPDA		VS-IMM JPDA	
	ToT%	FAR [l/(sm^2)]	ToT%	FAR [l/(sm^2)]
1	36.04	$0.656 \cdot 10^{-11}$	63.03	$1.401 \cdot 10^{-11}$
5	52.84	$1.266 \cdot 10^{-11}$	68.11	$1.769 \cdot 10^{-11}$
10	61.62	$1.681 \cdot 10^{-11}$	69.55	$1.997 \cdot 10^{-11}$

(b) S. Rossore

N^*	JPDA		VS-IMM JPDA	
	ToT%	FAR [l/(sm^2)]	ToT%	FAR [l/(sm^2)]
1	28.24	$0.2262 \cdot 10^{-11}$	55.92	$0.4169 \cdot 10^{-11}$
5	42.65	$0.4735 \cdot 10^{-11}$	58.62	$0.5985 \cdot 10^{-11}$
10	52.79	$0.6563 \cdot 10^{-11}$	60.58	$0.7445 \cdot 10^{-11}$

reported. Tracks generated from both the JPDA and VS-IMM JPDA are depicted in black, while the tracks generated only by the VS-IMM JPDA are depicted in red. No track is generated only by the standard JPDA. The results are obtained by using the parameter setting detailed before with $N^* = 5$. It is worth pointing out that thanks to the correct identification of the on-sea lane target dynamic, the KB-tracking is able to visibly reduce the N^{TF} and increase the ToT by properly propagating the track when no target-originated observations are received.

The first quantitative analysis is performed to show the improvements in terms of Time-on-Target (ToT). In Fig. 4, the daily ToT indexes are reported and obtained by averaging the results on all the on-sea lane targets per a certain day. The advantage of using the VS-IMM JPDA is clear: We have larger ToT for all the days on both the datasets. Generally speaking, the lower the probability to detect a target is, the greater is the improvement in terms of ToT. Hence, the improvement in terms of performance is more evident when N^* decreases, see Tab. I. Furthermore, the differences in ToT between the Palmaria and S. Rossore datasets are clear. Indeed, the ToT exhibited by S. Rossore is generally lower than the one on the Palmaria dataset (see, again, Tab. I), as already pointed out in [8].

The previous analysis lacks the contribution of the FAR. In order to have a fair comparison, we compare the ToT for both the approaches at fixed FAR values. This curve is obtained by varying the parameter N^*. Fig. 5 reports the convex hulls (solid lines) of daily couples (ToT,FAR) (square markers) for the compared approaches varying the N^* (assuming values in the range $[1, 10]$). The performance advantages are straightforward and, confirming the simulations, more evident in the low false alarm region. Furthermore, the improvements, for the case of S. Rossore, are better than the ones for Palmaria, because of a worse capability of the radar in S. Rossore to detect the vessels, see also [8]. An improvement of 10% on average is observed.

The last analysis is performed by exploiting the fragmentation index N^{TF}. In Tab. II, the daily values of the means and the standard deviations of the N^{TF} calculated for each day on all the on-sea lane tracks are shown. The overall means for Palmaria are 1.63 for JPDA and 1.32 for the VS-IMM, and 1.59 and 1.38, respectively, for S. Rossore. These outcomes confirm the capability of the KB-tracking to reduce the track fragmentation.

Finally, a computational analysis is performed. The elaboration times for both the compared approaches have been calculated on one day of data provided by Palmaria on May 17, 2009 using an Intel Xeon 3.73 GHz processor. We have that the VS-IMM JPDA requires 4754 s to be executed (*i.e.* 1.925 s per frame on average), while, the JPDA requires 4730 s (*i.e.* 1.915 s per frame on average). Practically, the two algorithms reach very close average elaboration times and only a little increase, due to the introduction of the IMM estimator, can be observed. However, in both the cases, the real-time requirement is guaranteed.

TABLE II. DAILY MEANS AND STANDARD DEVIATIONS OF N^{TF} INDEX FOR BOTH THE DATASETS.

(a) Palmaria

Date	JPDA	VS-IMM JPDA
	(μ,σ)	(μ,σ)
07/05	(1.18,0.40)	(1.29,0.49)
08/05	(1.62,0.83)	(1.40,0.65)
09/05	(1.67,1.17)	(1.36,0.49)
10/05	(1.86,1.28)	(1.45,0.89)
11/05	(1.67,1.24)	(1.60,1.12)
12/05	(1.65,0.71)	(1.43,0.60)
13/05	(1.89,1.19)	(1.59,0.89)
14/05	(1.56,0.93)	(1.16,0.47)
15/05	(1.52,0.82)	(1.17,0.39)
16/05	(1.77,1.41)	(1.39,0.79)
17/05	(1.52,1.29)	(1.16,0.50)
18/05	(1.42,0.69)	(1.29,0.69)
19/05	(1.66,0.94)	(1.23,0.53)
20/05	(1.33,0.82)	(1.50,0.58)
21/05	(1.43,0.77)	(1.00,0.00)
22/05	(1.69,1.16)	(1.14,0.36)
23/05	(1.96,1.51)	(1.46,0.90)
24/05	(1.57,0.79)	(1.26,0.45)
25/05	(1.75,1.07)	(1.39,0.70)
26/05	(1.62,0.95)	(1.27,0.56)
27/05	(1.75,1.36)	(1.50,0.88)
28/05	(1.62,1.01)	(1.27,0.46)
29/05	(1.50,1.05)	(1.37,0.88)
30/05	(1.83,1.62)	(1.33,0.96)
31/05	(1.61,1.46)	(1.24,0.56)
01/06	(1.45,0.94)	(1.13,0.35)
02/06	(1.65,1.23)	(1.18,0.39)
03/06	(1.90,1.72)	(1.28,0.70)
04/06	(1.75,1.29)	(1.37,0.56)

(b) S. Rossore

Date	JPDA	VS-IMM JPDA
	(μ,σ)	(μ,σ)
07/05	(1.13,0.35)	(1.13,0.35)
08/05	(1.67,0.99)	(1.37,0.56)
09/05	(1.82,1.33)	(1.41,0.80)
10/05	(1.31,0.60)	(1.12,0.34)
11/05	(1.38,0.87)	(1.23,0.83)
12/05	(1.64,1.15)	(1.36,0.63)
13/05	(1.62,0.96)	(1.31,0.60)
14/05	(1.60,0.83)	(1.43,0.65)
15/05	(2.11,1.76)	(1.32,0.58)
16/05	(1.78,1.44)	(1.58,0.84)
17/05	(1.48,0.59)	(1.35,0.57)
18/05	(1.13,0.35)	(1.00,0.00)
19/05	(1.27,0.46)	(1.07,0.26)
20/05	(1.00,0.00)	(1.00,0.00)
21/05	(1.62,0.51)	(1.33,0.49)
22/05	(1.69,0.87)	(1.35,0.61)
23/05	(1.79,0.80)	(1.64,0.74)
24/05	(1.44,0.63)	(1.50,0.65)
25/05	(1.72,1.07)	(1.50,1.03)
26/05	(2.56,1.98)	(2.24,1.82)
27/05	(1.87,1.54)	(1.56,0.96)
28/05	(1.47,0.64)	(1.20,0.41)
29/05	(1.65,1.11)	(1.35,0.79)
30/05	(1.50,0.89)	(1.44,0.63)
31/05	(1.56,0.73)	(1.37,0.52)
01/06	(1.40,0.52)	(1.30,0.48)
02/06	(1.83,1.15)	(1.78,1.11)
03/06	(1.24,0.75)	(1.19,0.54)
04/06	(1.86,1.46)	(1.50,0.94)

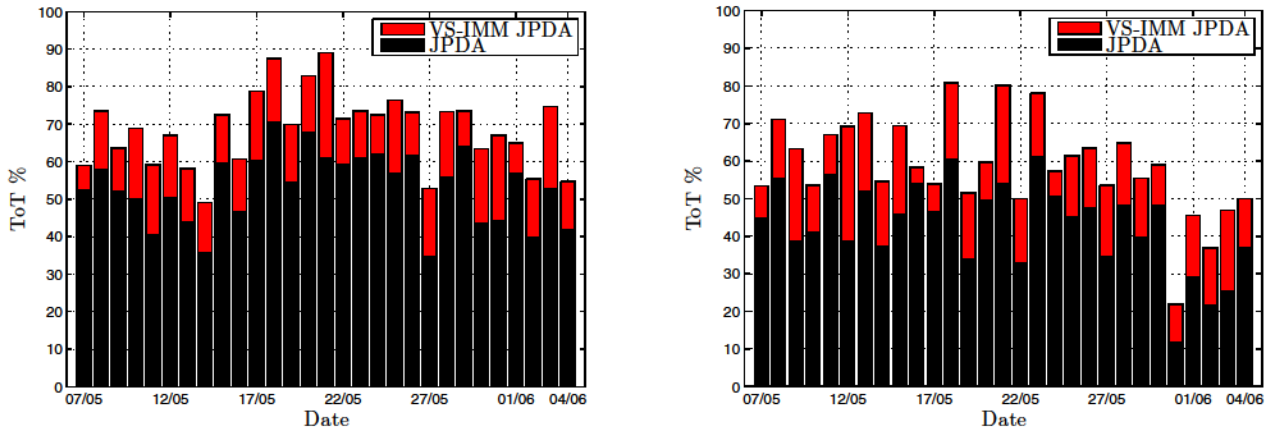

Fig. 4. Daily bar diagram for the ToT evaluated on the (a) Palmaria and (b) S. Rossore datasets. In this case, N^* is equal to 5.

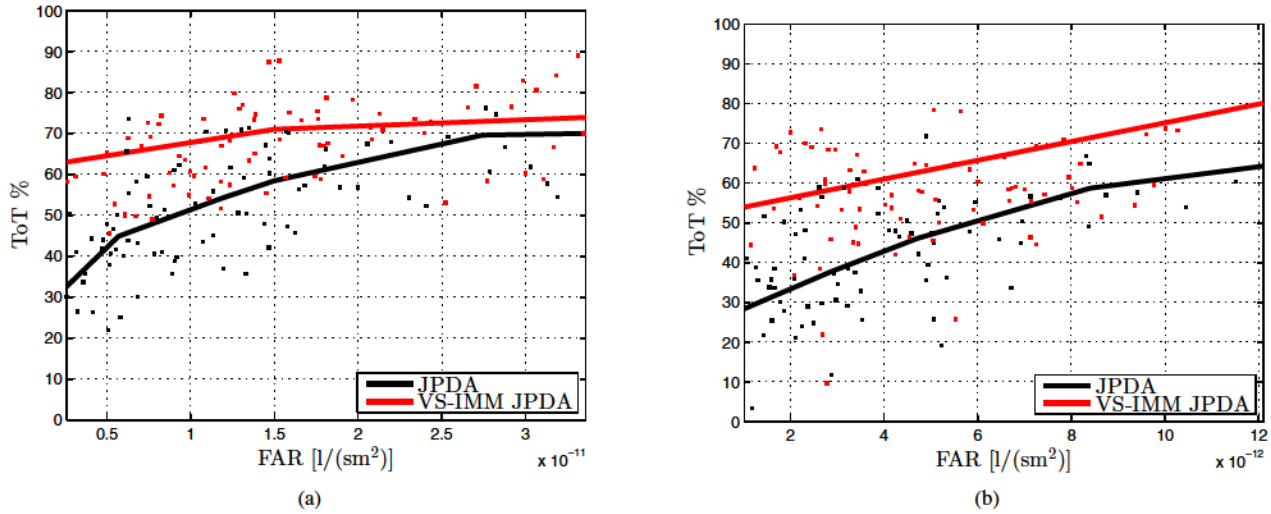

Fig. 5. ToT Vs. FAR varying N^* in the case of (a) Palmaria and (b) S. Rossore. Black and red little squares indicate the daily values for the standard JPDA and the VS-IMM JPDA, respectively.

IV. Conclusion

HFSW radars can be reliable long-range early-warning tools for maritime situational awareness applications. In this paper, a VS-IMM JPDA approach has been presented for tracking ships in a multi-target environment. More specifically, motion uncertainties due to on-sea lane/off-sea lane motion and sea lane entry/exit conditions have been managed. In addition, obscuration of the targets, due to the radar synchronization and first order Bragg scattering reasons, has been also handled.

Experimental results from both simulated data and one month of real data acquired by two HFSW radars have been presented. The advantages, in terms of, time-on-target, false alarm rate, and track fragmentation of the proposed VS-IMM JPDA with respect to the standard JPDA [8] have been shown and confirmed by AIS data used as ground-truth. The better capability of the proposed approach of following targets without increasing the false alarm rate has been shown. This increment in the time-of-target index can be over the 30% in some regions for both the HFSW systems. Finally, we also obtain an average reduction in track fragmentation of about the 20% and the 13% for Palmaria and S. Rossore, respectively.

Acknowledgment

The authors wish to thank the NATO Allied Command Transformation (NATO-ACT) for supporting the research activity of the Centre for Maritime Research and Experimentation (CMRE) Maritime Situational Awareness (MSA) project.

References

[1] S. Grosdidier, A. Baussard, and A. Khenchaf, "HFSW radar model: Simulation and measurement," *IEEE Trans. Geosci. Remote Sens.*, vol. 48, no. 9, pp. 3539–3549, Sep. 2010.

[2] K.-W. Gurgel, A. Dzvonkovskaya, T. Pohlmann, T. Schlick, and E. Gill, "Simulation and detection of tsunami signatures in ocean surface currents measured by HF radar," *Ocean Dyn., Springer Berlin/Heidelberg*, vol. 61, no. 10, pp. 1495–1507, Oct. 2011.

[3] D. Barrick, "History, present status, and future directions of HF surface-wave radars in the US," in *Proc. of the IEEE Radar Conf.*, Sep. 2003, pp. 652–655.

[4] D. E. Barrick and M. W. Evans, "Implementation of coastal current-mapping HF radar system," *NOAA*, no. 1, Jul. 1976.

[5] K.-W. Gurgel, G. Antonischki, H.-H. Essen, and T. Schlick, "Wellen radar (WERA), a new ground-wave based HF radar for ocean remote sensing," *Coastal Eng.*, vol. 37, no. 3, pp. 219–234, Aug. 1999.

[6] S. Maresca, M. Greco, F. Gini, R. Grasso, S. Coraluppi, and N. Thomas, "The HF surface wave radar WERA. part I: Statistical analysis of recorded data," in *Proc. of the IEEE Radar Conf.*, Washington, USA, May 2010.

[7] ——, "The HF surface wave radar WERA. part II: Spectral analysis of recorded data," in *Proc. of the IEEE Radar Conf.*, Washington, USA, May 2010.

[8] S. Maresca, P. Braca, J. Horstmann, and R. Grasso, "Maritime surveillance using multiple high-frequency surface-wave radars," *IEEE Trans. Geosci. Remote Sens.*, vol. 52, no. 8, pp. 5056–5071, Aug. 2014.

[9] A. Dzvonkovskaya, K.-W. Gurgel, H. Rohling, and T. Schlick, "Low power high frequency surface wave radar application for ship detection and tracking," in *Proc. of the IEEE Radar Conf.*, Vilnius, Lithuania, Sep. 2010.

[10] Y. Bar-Shalom, F. Daum, and J. Huang, "The probabilistic data association filter," *IEEE Control Syst. Mag.*, vol. 29, no. 6, pp. 82–100, Dec. 2009.

[11] Y. Bar-Shalom, P. Willett, and X. Tian, *Tracking and Data Fusion: A Handbook of Algorithms*. Storrs, CT: YBS Publishing, Apr. 2011.

[12] S. J. Julier and J. K. Uhlmann, "Unscented filtering and nonlinear estimation," *Proc. IEEE*, vol. 92, no. 3, pp. 401–422, Mar. 2004.

[13] T. Kirubarajan, Y. Barshalom, K. Pattipati, and I. Kadar, "Ground target tracking with variable structure IMM estimator," *IEEE Trans. Aerosp. Electron. Syst.*, vol. 36, no. 1, pp. 26–46, Jan. 2000.

[14] Z. Duan, C. Han, and X. R. Li, "Sequential nonlinear tracking filter with range-rate measurements in spherical coordinates," in *Proc. of the* 7^{th} *International Conference on Information Fusion (FUSION)*, Stockholm, Sweden, Jun. 2004.

[15] L. Bruno, P. Braca, J. Horstmann, and M. Vespe, "Experimental evaluation of the range-Doppler coupling on HF surface wave radars," *IEEE Geosci. Remote Sens. Lett.*, vol. 10, no. 4, pp. 850–854, Jul. 2013.

[16] G. Vivone, P. Braca, and J. Horstmann, "Knowledge-based multitarget ship tracking for HF surface wave radar systems," *IEEE Trans. Geosci. Remote Sens.*, 2015.

[17] P. Braca, R. Grasso, M. Vespe, S. Maresca, and J. Horstmann, "Application of the JPDA-UKF to HFSW radars for maritime situational awareness," in *Proc. of the* 15^{th} *Intern. Conf. on Inform. Fusion (FUSION)*, Singapore, Jul. 2012.

[18] B. Chen and J. Tugnait, "Tracking of multiple maneuvering targets in clutter using IMM/JPDA filtering and fixed-lag smoothing," *ELSEVIER Automatica*, vol. 37, no. 2, pp. 239–249, Feb. 2001.

Document Data Sheet

Security Classification		Project No.
Document Serial No.	**Date of Issue**	**Total Pages**
CMRE-PR-2019-132	June 2019	8 pp.

Author(s)

Gemine Vivone, Paolo Braca, Jochen Horstmann

Title

Variable structure interacting multiple model algorithm for ship tracking using HF surface wave radar data

Abstract

These last decades spawned a great interest towards low-power High-Frequency (HF) Surface-Wave (SW) radars for ocean remote sensing. By virtue of their over-the-horizon coverage capability and continuous-time mode of operation, these sensors are also effective long-range early-warning tools in maritime situational awareness applications. In this paper we show how it is possible to take advantage of a priori information on traffic by the means of a knowledge-based multi-target tracking algorithm, demonstrating that the tracking stage can be enhanced by combining on-line data from the HFSW radar with ship traffic information. A significant improvement of the proposed procedure, in terms of system performance, is demonstrated in comparison with the state-of-the-art approach recently presented in the literature. The main benefit of our approach is the ability to better follow targets without increasing the false alarm rate. The ability to follow targets can be over 30% better than existing methods. The proposed approach also exhibits a reduction of the track fragmentation. Average gains between the 13% and the 20% are observed.

Keywords

Radar tracking , target tracking, marine vehicles, sea measurements, noise, standards

Issuing Organization

NATO Science and Technology Organization
Centre for Maritime Research and Experimentation

Viale San Bartolomeo 400, 19126 La Spezia, Italy

[From N. America:
STO CMRE
Unit 31318, Box 19, APO AE 09613-1318]

Tel: +39 0187 527 361
Fax:+39 0187 527 700

E-mail: library@cmre.nato.int